TU Delft

Delft University of Technology

An Investigation of Carburization Behavior of Molten Iron for the Flash Ironmaking Process

Wang, Qiang; Li, Guangqiang; Zhang, Wei; Yang, Yongxiang

DOI
10.1007/s11663-019-01594-0

Publication date
2019

Document Version
Final published version

Published in
Metallurgical and Materials Transactions B: Process Metallurgy and Materials Processing Science

Citation (APA)
Wang, Q., Li, G., Zhang, W., & Yang, Y. (2019). An Investigation of Carburization Behavior of Molten Iron for the Flash Ironmaking Process. *Metallurgical and Materials Transactions B: Process Metallurgy and Materials Processing Science*, *50*(4), 2006-2016. https://doi.org/10.1007/s11663-019-01594-0

Important note
To cite this publication, please use the final published version (if applicable).
Please check the document version above.

Copyright
Other than for strictly personal use, it is not permitted to download, forward or distribute the text or part of it, without the consent of the author(s) and/or copyright holder(s), unless the work is under an open content license such as Creative Commons.

Takedown policy
Please contact us and provide details if you believe this document breaches copyrights.
We will remove access to the work immediately and investigate your claim.

This work is downloaded from Delft University of Technology.
For technical reasons the number of authors shown on this cover page is limited to a maximum of 10.

An Investigation of Carburization Behavior of Molten Iron for the Flash Ironmaking Process

QIANG WANG, GUANGQIANG LI, WEI ZHANG, and YONGXIANG YANG

In order to recognize the dripping and the carburizing behaviors of the molten iron within the coke packed bed in the flash ironmaking process, a transient three-dimensional numerical model was developed. The volume of fluid (VOF) approach is used to describe the movement of the molten iron and the argon gas. The porous medium module is employed to define the momentum, heat, and mass transfer between the coke packed bed and the molten iron. Moreover, a factor is introduced to consider the influence of the ash film on the carburization process. A reasonable agreement between the experiment and simulation is obtained. The results indicate that the molten iron flows downward from the upper crucible to middle crucible. After entering the middle crucible, the molten iron spreads around within the coke packed bed and simultaneously moves downward. The carbon is, therefore, transferred from the coke to the molten iron. With the 47-mm-height coke packed bed, the carbon content in the molten iron after the carburization decreases from 3.19 to 1.97 pct, while the coke diameter ranges from 2 to 5 mm. With the 2-mm-diameter coke, the carbon content in the molten iron after the carburization increases from 2.84 to 4.81 pct, while the coke packed bed height increases from 37 to 97 mm.

https://doi.org/10.1007/s11663-019-01594-0
© The Minerals, Metals & Materials Society and ASM International 2019

I. INTRODUCTION

In order to reduce the energy consumption and greenhouse gas carbon dioxide emissions during the ironmaking process, many alternating technologies, such as direct-reduced iron and smelting reduction, have been proposed.[1,2] A novel, high-intensity flash ironmaking process is now under development.[3–5] During this process, the iron ore concentrate is flash reduced by gaseous reductants at temperatures above 1423 K (1150 °C). The oxygen in the iron ore concentrate can be efficiently removed, and a higher purity iron is, therefore, obtained. Since the mass transfer of the carbon between the gaseous reduction and the iron ore concentrate is limited, the carbon content in the reduced iron is negligible. However, the favorable carbon content in the molten iron for the converter steelmaking ranges from 3 to 4 pct.[6,7] For achieving the appropriate carbon content, a carburizing process of the reduced iron is, thus, implemented by using a coke packed bed. The reduced iron is first melted and then travels through the coke packed bed, and is finally collected.

To successfully control the carburizing process, it is essential to recognize the mechanism and kinetics of the dissolution of the coke into the molten iron. Various investigations about the iron carburization have been reported.[8–13] It has been generally considered that the dissolution of carbon from the carbonaceous materials is a two-step process. The first step includes the dissociation of carbon atoms from their crystal site in the carbonaceous materials into the carbon-melt interface. The second step is the mass transfer of carbon atoms through the adjacent boundary layer into the bulk of the molten iron. Furthermore, the second step, *i.e.*, the diffusion of the carbon within the molten iron, has been shown to be the rate-limiting step, and a first-order kinetic equation was proposed to describe the mass transfer of the carbon. The type of the carbonaceous material also influences the carbon pickup of the molten iron. The dissolution of the carbon from the coke is proved to be much slower than that from the graphite. The reduction in the dissolution rate is attribute to the presence of the ash, which reduces the

QIANG WANG and YONGXIANG YANG are with The State Key Laboratory of Refractories and Metallurgy, Wuhan University of Science and Technology, Wuhan, 430081 Hubei, P.R. China, with the Key Laboratory for Ferrous Metallurgy and Resources Utilization of Ministry of Education, Wuhan University of Science and Technology, and also with Department of Materials Science and Engineering, Delft University of Technology, Mekelweg 2, 2628 CD Delft, The Netherlands. GUANGQIANG LI and WEI ZHANG are with The State Key Laboratory of Refractories and Metallurgy, Wuhan University of Science and Technology, and also with the Key Laboratory for Ferrous Metallurgy and Resources Utilization of Ministry of Education, Wuhan University of Science and Technology. Contact emails: liguangqiang@wust.edu.cn; wei_zhang@wust.edu.cn
Manuscript submitted December 10, 2018.
Article published online May 17, 2019.

carbon pickup by covering the coke surface and preventing direct contact between the carbon and the molten iron.

Generally, experiments were carried out to explore the carbon transfer behavior by taking periodic samples of the molten iron or by determining the weight loss from the carbonaceous material.[14] From the data obtained, a carbon content in molten iron and time, the value of the mass transfer rate is determined. Nevertheless, the carbon transfer behavior is also significantly affected by the flow of the molten iron.[10,15] The molten iron can only flow through the voids in the coke packed bed if the fluid capillary pressure at the void neck can be overcome. The size of the coke as well as the packed bed structure is supposed to influence the flow pathway of the molten iron and the carbon migration behavior. It is tough to know exactly the flow pattern of the molten iron within the coke packed bed only through experiments because of the high temperature and the opaque container. Together with the development of more advanced numerical techniques and higher computer performance, the computational fluid dynamics (CFD) approach becomes a powerful tool in understanding the characteristics of the molten iron flow since the CFD can provide comprehensive data.

In the current investigation, a transient three-dimensional numerical model was established to represent the dripping and the carburizing behavior of the molten iron within the coke packed bed and to study the influences of the diameter of the coke and the height of the coke packed bed on the mass transfer of the carbon. At the same time, necessary measurement is also required to validate the developed model. A series of experiments were, therefore, conducted by using a high-temperature coke packed bed.

II. EXPERIMENTAL PROCEDURE

The experimental apparatus is shown in Figure 1. The crucible assembly is placed in the center of the alumina reaction tube in a silicon-molybdenum electric resistance furnace filled with a 99.999 pct purity argon gas. The crucible assembly consists of three alumina crucibles with the same inner diameter of 64 mm. About 900 grams of the solid pieces of the electrolytic iron with 99.99 pct purity are placed in the upper crucible. There is a 10-mm-diameter hole at the center of the bottom of the upper crucible, and in order to prevent the fall of the electrolytic iron pieces, an alumina disk with 15-mm diameter and 4-mm thickness is employed to cover the hole. The middle crucible is then filled with coke, the composition of which is shown in Table I. Different sizes of the coke and the middle crucible are used in the experiments in order to study the influences of the diameter of the coke and the height of the coke packed bed. The mean diameter of the coke and the inside height of the middle crucible ranges from 2 to 5 mm and from 37 to 97 mm, respectively. Besides, 10 outlets with 3-mm diameter are uniformly distributed at the base of the middle crucible. The bottom crucible is served as a receiver to hold the molten iron after the carburization.

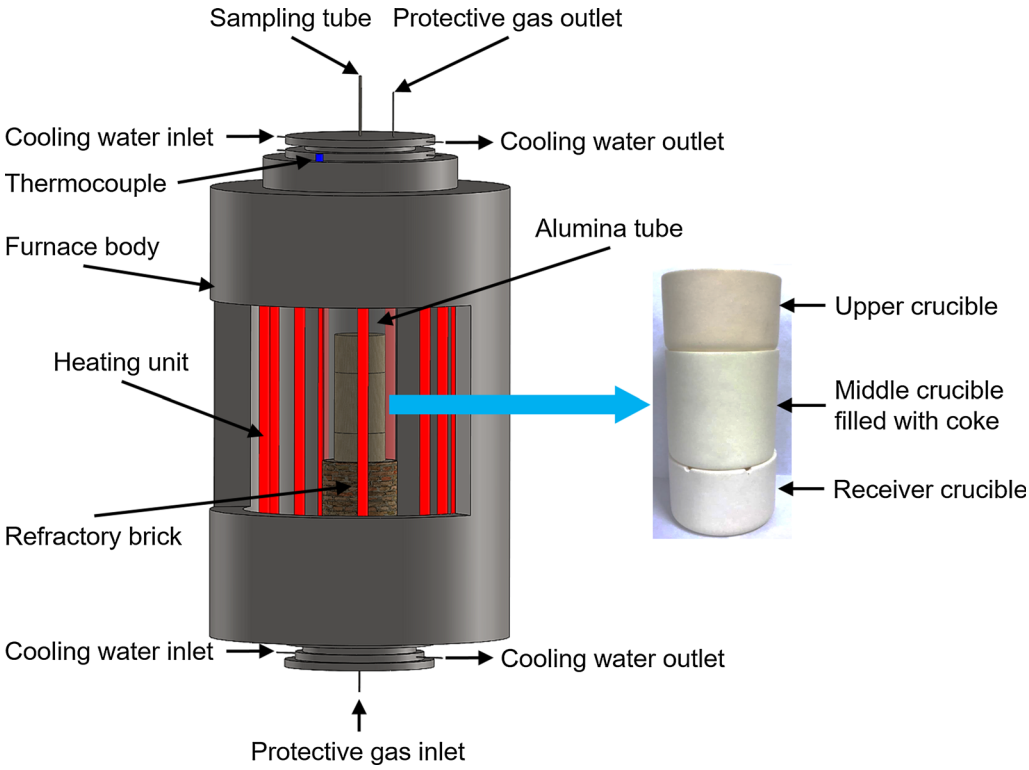

Fig. 1—Schematic illustration of the experimental apparatus.

Table I. Chemical Composition of the Coke

Component	Content (Wt Pct)
Fixed Carbon	85.31
Ash (Mainly SiO_2)	13.37
Volatile Matter	0.92
Sulfur	0.35
Moisture	0.05

By flowing the argon gas at a rate of 5 NL/min, the furnace is heated to 1873 K (1600 °C) at a heating rate of 10 K/min. The flow rate of the argon gas is then changed to 2 NL/min after the desired temperature is reached. The crucible assembly is placed into a larger graphite crucible and then is put together concentrically into the heating zone of the furnace on a refractory stand of a required height by using a crucible tong. The solid pieces of the electrolytic iron are rapidly melted, and the alumina disk immediately floats upward. Afterward, the molten iron flows into the coke packed bed through the hole at the bottom of the upper crucible. The carburized molten iron in the bottom crucible is eventually cooled inside the furnace to room temperature. The carbon concentration in the final solidified iron is measured using a carbon sulfur analyzer.

III. MATHEMATICAL MODEL

A. *Assumptions*

The following assumptions are proposed to simplify the model.

1. The computational domain includes the upper crucible (fluid medium) and the middle crucible (porous medium), as illustrated in Figure 2.[16]
2. The argon gas and the molten iron are taken into account in the simulation, and the two fluids are incompressible Newtonian fluid. The density of the molten iron is a function of the carbon content. The other properties of the argon gas and the molten iron are assumed to be constant.
3. The heat transfer is not included in the simulation, and the temperature is assumed to be 1873 K (1600 °C).
4. The coefficient of the interfacial tension between the metal and the slag remains the same.
5. Other elements in the molten iron are ignored, except the carbon.

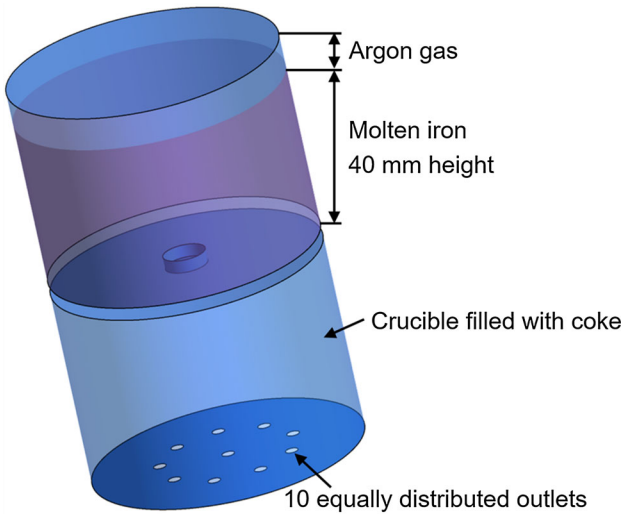

Fig. 2—Schematic illustration of the computational domain.

B. *Volume of Fluid Method*

For modeling the two-phase flow of the argon gas and the molten iron, the volume of fluid (VOF) method is adopted to track a scalar field variable α, namely, volume fraction, in the entire domain:[17]

$$\frac{\partial \alpha}{\partial t} + \nabla \cdot (\vec{v}\alpha) = 0 \qquad [1]$$

In the present work, α stands for the volume fraction of the molten iron and is updated at every time-step. t indicates the time, and $\vec{v}$ means velocity. Meanwhile, the properties of the mixture phase, $\bar{\varphi}$, are related to the volume fraction:

$$\bar{\varphi} = \varphi_{\mathrm{m}}\alpha + \varphi_{\mathrm{g}}(1-\alpha) \qquad [2]$$

where φ_m and φ_g are the properties of the molten iron and the argon gas, respectively. The interfacial tension between the argon gas and the molten iron is estimated by the continuum surface force module.[18]

C. *Fluid Flow*

The flow is described with the mass continuity and time-averaged Navier–Stokes equations:[19]

$$\frac{\partial \bar{\rho}}{\partial t} + \nabla \cdot (\bar{\rho}\vec{v}) = 0 \qquad [3]$$

$$\frac{\partial (\bar{\rho}\vec{v})}{\partial t} + \bar{\rho}\vec{v} \cdot \nabla \vec{v} = -\nabla p + \nabla \cdot \left(\mu_{eff}\nabla \vec{v}\right) + \vec{F} \qquad [4]$$

where $\bar{\rho}$ is the density of the mixture phase, p is the pressure, and μ_{eff} is the effective viscosity. The last term, $\vec{F}$, on the right side of Eq. [4] is an additional friction term due to the porous medium. As mentioned previously, we treat the coke packed bed as a homogeneous porous medium, and the momentum loss of the molten iron in the coke packed bed can be represented by

$$\vec{F} = -\left(\frac{\overline{\mu}}{\phi}\vec{v} + C\frac{1}{2}\bar{\rho}|\vec{v}|\vec{v}\right) \qquad [5]$$

where $\bar{\mu}$ is the dynamic viscosity of the mixture phase, ϕ is the void ratio of the coke packed bed, and C is the inertial resistance factor. The first part of the previous equation on the right side is Darcy's law, which accounts for the microscopic viscous drag. The second part expresses the inertial loss due to the strong geometrical variation of the streamlines at the pore scale.

The movement of the molten iron and the argon gas is weakly turbulent in the crucible used in the experiments. The standard k–ε turbulence model is developed for flows with a high Reynolds number and does not meet the situation here. The RNG k–ε turbulence model, which is able to capture the behavior of flows with lower Reynolds numbers, is therefore employed to calculate the turbulent viscosity. An enhanced wall function is also invoked to work with the RNG k–ε turbulence model.

D. *Mass Transfer of Carbon*

The carbon in the coke will be dissolved into the molten iron, as mentioned previously. Meanwhile, the convection and the diffusion of the carbon in the molten iron also promote the carbon pickup. These phenomena are described by[15,16]

$$\frac{\partial}{\partial t}(\phi\rho_{\mathrm{m}}c) + \nabla\cdot(\phi\rho_{\mathrm{m}}\vec{v}c) = \nabla\cdot\left(D_{\mathrm{c,m}}\nabla c\right) + S_{\mathrm{r}} \quad [6]$$

where c is the carbon concentration in the molten iron and $D_{\mathrm{c,m}}$ is the diffusion coefficient of carbon in the molten iron. The preceding mass transfer equation is applied to the molten iron.

The carburization reaction is represented by the source S_{r}, and a first-order reaction rate is employed to define the carbon transfer behavior:[20]

$$S_{\mathrm{r}} = \frac{k\cdot nA}{V}(c_s - c_t) \quad [7]$$

where c_s and c_t are the saturation carbon solubility and the carbon content at time t, respectively. The driving force for the carbon dissolution is the value of the difference at any instant between the saturation value of the carbon and the actual carbon content in the molten iron, *i.e.*, $(c_s - c_t)$. The saturation value of the carbon is set as 6.69 pct and is kept constant in the simulation. k denotes the rate constant, A is the interfacial contact area between the coke and the molten iron, and V is the volume of the molten iron. Besides, we introduce a factor, n, which represents the effective coke surface area and is termed "ash factor."[21] The importance of this factor is that it indicates to what extent the coke surface area is available for the chemical reaction. A value of 1 implies that all the surface area of the coke can be used for the carbon dissolution, that is, no ash film is formed on the surface of the coke to prevent the carbon pickup. The ash factor changes over the dissolution time:[8]

$$n = e^{(-\lambda\cdot d_c\cdot t)} \quad [8]$$

where λ is a coefficient and is determined by our experiments. d_c is the mean diameter of the coke.

E. *Boundary Conditions*

Figure 3 depicts the boundaries and the mesh model used in the simulation. The grid pattern here is coarsely displayed to aid reader visualization.

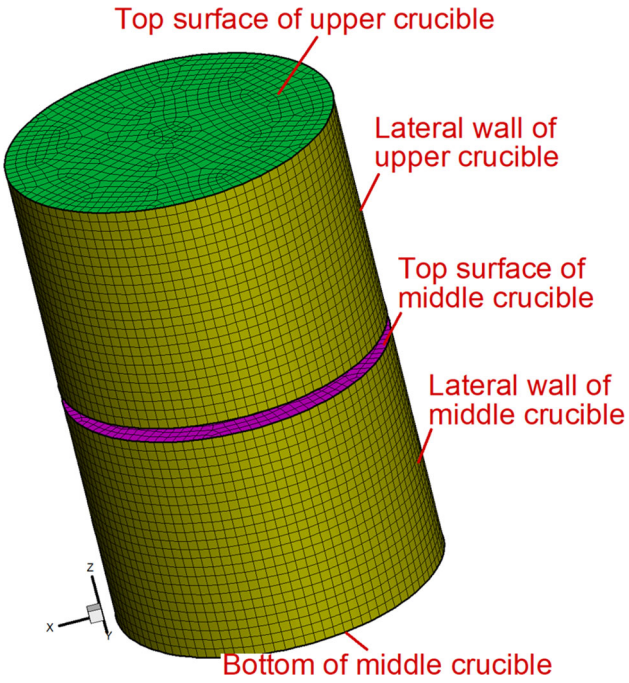

Fig. 3—Boundaries and mesh model used in the simulation.

Since the crucible assembly is placed in the electric resistance furnace filled with argon gas, the pressure inlet boundary condition is used at the top surfaces of the upper and the middle crucibles, and the value is equal to 1 bar. The molten iron is allowed to flow out of the computational domain through the 10 equally distributed outlets at the bottom of the middle crucible, and the pressure here is also equal to 1 bar. Other walls are assumed to obey the no-slip wall boundary condition.

The carbon transfer between the coke packed bed and the molten iron is assumed to occur within the middle crucible. The carbon is allowed to leave the computational domain along with the flow of the molten iron, while it is forbidden to move at the lateral wall and the bottom of the middle crucible. The detailed physical properties of the molten iron and argon gas and the model parameters are listed in Table II.[8,14,21–23]

IV. SOLUTION PROCEDURE

The control-volume-based technique is used to convert the governing equations for the momentum and mass transfers that can be solved numerically. The discretization of these equations and their solutions is solved by means of the segregated solver, which is provided by the commercial software ANSYS Fluent 14.5. Also, the introduction of the rate of the carburization reaction between the coke and the molten iron is achieved by our own program. Through the application of the user-defined function, our own program is interpolated into the commercial numerical code. The required quantities for our own program, such as carbon content, interfacial area, and time, are provided

Table II. Physical Properties of the Molten Iron and Argon Gas and the Model Parameters

Parameter	Value
Physical Properties of Molten Iron	
Density (kg/m^3)	$6910 - 69.6 \times c_t$
Dynamic Viscosity (Pa s)	1.96×10^{-3}
Diffusion Coefficient of Carbon (m^2/s)	3.03×10^{-15}
Physical Properties of Argon Gas	
Density (kg/m^3)	0.399
Dynamic Viscosity (Pa s)	2.1×10^{-5}
Interfacial Tension Coefficient Between Argon Gas and Molten Iron (N/m)	1.192
Model Parameters	
Mean Diameter of Coke (mm)	2/3/4/5
Void Ratio of Coke Packed Bed	0.422/0.451/0.479/0.511
Height of Coke Packed Bed (mm)	37/47/77/97
Rate Constant Used in Eq. [7] (m/s^2)	1.6×10^{-2}
Coefficient Used in Eq. [8]	18.28

by the commercial numerical code; then the calculated mass transfer rate of the carbon is returned to the commercial numerical code.

A standard pressure interpolation scheme is required to compute the face values of pressure from the cell values. The SIMPLE algorithm is applied in pressure-velocity coupling in the segregated solver to adjust the velocity fields by correcting the pressure field. The second order upwind scheme is chosen to determine each governing equation for a higher accuracy. Before advancing, the iterative procedure continues until all normalized unscaled residuals are less than 10^{-6}.

A structured mesh is created to discretize the physical domain with the respective sizes of 0.5, 0.6, and 0.9 mm. The grid independence test is then conducted. After a typical simulation, the velocity and the carbon content of some points in the domain are carefully compared. The deviation of simulated results between the first and second mesh is about 4 pct, while it is approximately 9 pct between the second and third mesh. Considering the high expense of computation, we retain the second mesh to use throughout the rest of this work. One typical simulation takes approximately 165 CPU hours by using eight cores of 4 GHz and a 0.01-second time-step.

V. RESULTS AND DISCUSSION

A. *Fluid Flow*

Figure 4 shows the distribution of the volume fraction of the molten iron at different moments. The mean diameter of the coke in this scenario is 2 mm, and the height of the coke packed bed is 47 mm. At the beginning, the molten iron is in the upper crucible and the height of the molten iron is 40 mm. The space above the molten iron in the upper crucible and the void space among the coke packed bed in the middle crucible are filled with the argon gas.

We can see clearly that the molten iron flows downward under the action of gravity and enters the middle crucible through the hole at the center of the bottom of the upper crucible. Some argon gas will be caught by the molten iron when the molten iron passes through the hole, and this argon gas then adheres to the lateral wall of the hole due to the pressure of the molten iron, as illustrated in Figure 4(a). The molten iron spreads around within the coke packed bed after entering the middle crucible and simultaneously moves downward, as displayed in Figure 4(b). When the molten iron travels to the bottom of the middle crucible, it then flows out of the domain through the 10 equally distributed outlets, as demonstrated in Figures 4(c) and (d). Since the total area of the 10 outlets is a little less than the cross-sectional area of the hole, the molten iron accumulates in the lower part of the middle crucible. The height of the molten iron in the coke packed bed, therefore, gradually increases and finally remains stable, as shown in Figures 4(e) and (f). The coke packed bed is partly filled by the molten iron. With the continuous dripping of the molten iron, almost all molten iron comes into the coke packed bed. There is only a small amount of molten iron residue on the flat base of the upper crucible. The argon gas bubble is involved in the molten iron and moves downward along with the molten iron, as seen in Figure 4(g). Due to the resistance of the coke packed bed, the continuous stream of the molten iron is broken into several drops of the molten iron, as shown in Figure 4(h). During the flowing, the molten iron droplets can only pass and access a void if the fluid capillary pressure at the void neck can be overcome. Most of the molten iron eventually flows out of the coke packed bed from the 10 equally distributed outlets at the bottom of the middle crucible. Similarly, there is little molten iron residue within the coke packed bed at the bottom, as displayed in Figure 4(i). The entire dripping process of the molten iron takes approximately 6.03 seconds. It can be seen that the molten iron, flowing down along the accessible void, uses part of the coke packed bed. The residence time of the molten iron in the coke packed bed depends on the length of the pathway and is a function of the diameter of the coke and the height of the coke packed bed.

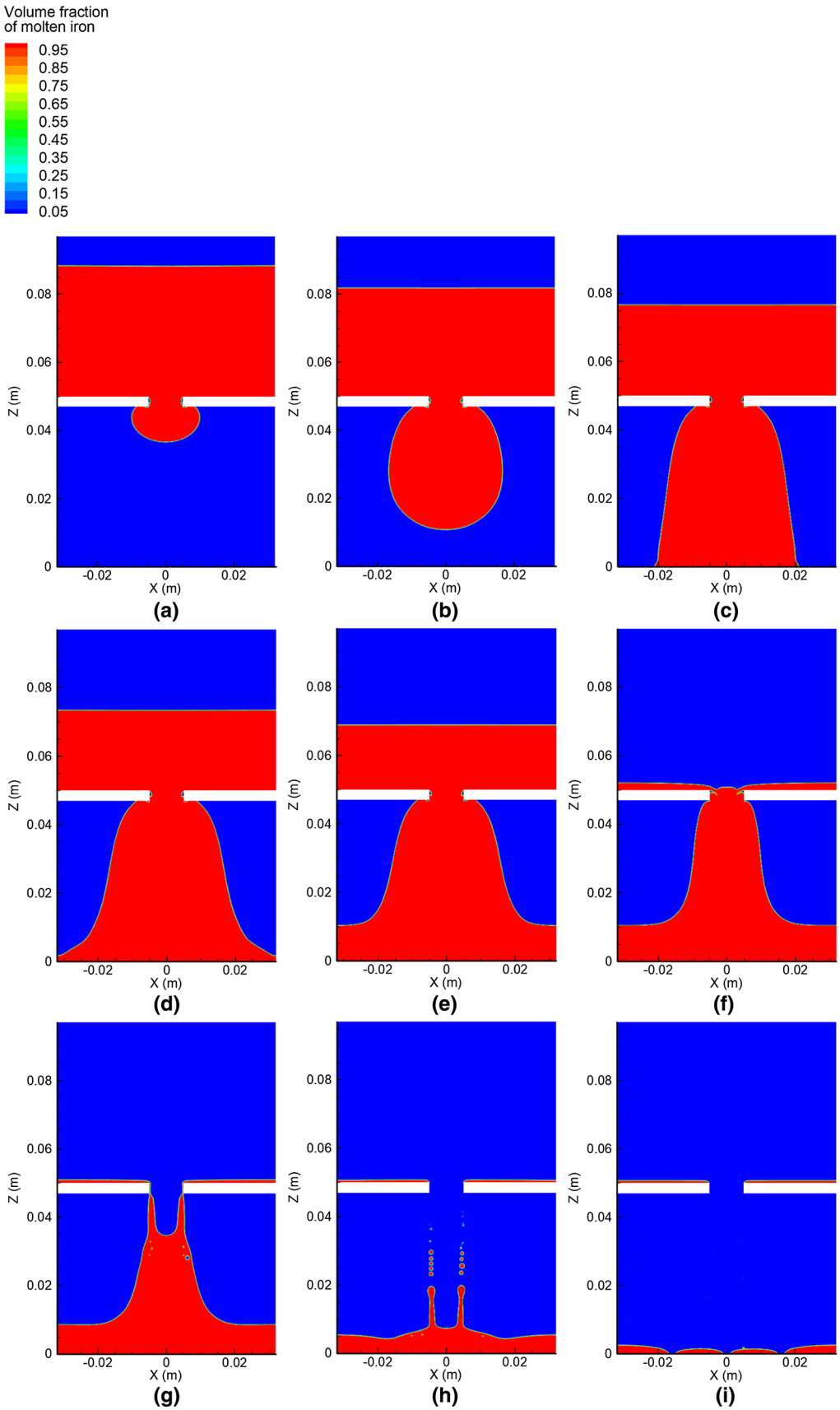
Volume fraction
of molten iron
0.95
0.85
0.75
0.65
0.55
0.45
0.35
0.25
0.15
0.05
Z (m)
X (m)
0
0.02
0.04
0.06
0.08
-0.02
0
0.02
(a)
(b)
(c)
(d)
(e)
(f)
(g)
(h)
(i)

◀Fig. 4—Distribution of the molten iron volume fraction at different moments. (*a*) t_0 s, (*b*) t_0 + 0.34 s, (*c*) t_0 + 0.64 s, (*d*) t_0 + 0.84 s, (*e*) t_0 + 1.14 s, (*f*) t_0 + 2.69 s, (*g*) t_0 + 3.04 s, (*h*) t_0 + 3.54 s, and (*i*) t_0 + 4.04 s. The mean diameter of the coke is 2 mm, and the height of the coke packed bed is 47 mm.

B. *Transfer Behavior of Carbon*

Figure 5 indicates the variation of the distribution of the carbon content in the molten iron. It can be seen that the concentration of the carbon at the front of the stream of the molten iron gradually increases while flowing down, since the carbon is continuously transferred from the coke to the molten iron. The highest concentration of the carbon, around 6.21 pct, is found at the outside corner of the middle crucible, because the outside corner of the middle crucible is a dead zone and the move of the molten iron is slow. More opportunities, therefore, can be provided for the carbon migration.

Figure 6 shows the variation of the average mass fraction of the carbon and the total mass flow rate of the molten iron at the 10 outlets. The mass flow rate rapidly increases at around 0.55 seconds, reaches the maximal value at approximate 1.72 seconds, and then gradually decreases over time. The evolution of the average carbon mass fraction, however, tells a different story. The carbon content first rises fast due to the draining out of the molten iron and then enters a relatively stable period. The change of the mass transfer rate of the carbon between the coke and the molten iron is small during this time. The carbon content attains the maximal value at about 4.03 seconds, as the molten iron at the bottom periphery of the middle crucible flows out. Afterward, the carbon content decreases with time. Furthermore, the curve of the carbon content is zigzag rather than smooth as before. The mixture of the molten iron with different carbon concentrations at the bottom of the coke packed bed can be responsible for this phenomenon. The average carbon concentration at the 10 outlets increases when the molten iron with a higher carbon content moves to the outlets and quickly reduces if the molten iron with a lower carbon content travels to the outlets.

C. *Effect of the Diameter of the Coke*

As mentioned in Section B, the carburization of the molten iron is influenced by the diameter of the coke and the height of the coke packed bed. Figure 7 shows the effect of the diameter of the coke on the total mass flow rate of the molten iron at the 10 outlets. The height of the coke packed bed is kept at 47 mm. We can see that the residence time of the molten iron in the coke packed bed decreases from 6.03 to 3.45 seconds with the coke diameter ranging from 2 to 5 mm. The main reason can be attributed to the decreasing resistance of the coke packed bed.

Figure 8 displays the effect of the diameter of the coke on the average mass fraction of the carbon at the 10 outlets. The variations of the carbon concentration with different coke diameters are basically the same. The carbon content first quickly rises and then remains relatively stable. After that, the carbon content rises again and a peak value of the carbon content is observed. The carbon content finally decreases to zero.

The peak value of the carbon content drops from 6.21 to 4.07 pct when the coke diameter changes from 2 to 5 mm, which suggests that the mass transfer of the carbon between the coke and the molten iron is reduced, mainly because the specific surface area of the coke tends to decrease with a larger diameter. The reaction area for the carburization decreases as well. Furthermore, the influence of the ash film cover on the surface of the coke also increases with the growing size of the coke according to Eq. [8].

Figure 9 depicts the mass fraction of the carbon in the molten iron after the carburization. Less carbon is transferred from the coke to the molten iron with the increasing coke diameter, as discussed previously. Also, the impact of the coke diameter on the mass transfer of the carbon increases. The carbon content in the molten iron decreases from 3.06 to 2.31 pct when the coke diameter changes from 3 to 4 mm, and the decreasing amplitude of the carbon content reaches the maximum value, around 24.5 pct, under this circumstance. As mentioned previously, the favorable carbon content in the molten iron for the converter steelmaking ranges from 3 to 4 pct. From the result, we can see that the cokes with 4- and 5-mm diameters cannot achieve the target of the carburization if the height of the coke packed bed is kept at 47 mm.

We also measured the carbon content in the molten iron after the carburization and compared it with the simulated data. It is found that the present simulation results match closely with the experimental data, and the deviation is within acceptable limits. The agreement lends confidence in the fundamental validity of the developed model.

D. *Effect of the Height of the Coke Packed Bed*

Figure 10 shows the effect of the height of the coke packed bed on the total mass flow rate of the molten iron at the 10 outlets. The diameter of the coke in the four scenarios is 2 mm. The change rule of the total mass flow rate of the molten iron with different coke packed bed heights remains unchanged. Moreover, the peak values of the four curves are almost the same. With the increasing height of the coke packed bed, the residue time of the molten iron in the coke packed bed increases from 5.93 to 6.79 seconds.

Due to a longer residue time, more carbon can be transferred to the molten iron from the coke, as shown in Figure 11. The peak value of the carbon content variation curve increases from 5.78 to 6.61 pct, while the height of the coke packed bed ranges from 37 to 97 mm. The occurrence time of the peak is also put off because of the higher coke packed bed.

The carbon concentration in the molten iron after the carburization, therefore, increases with the higher coke packed bed, as demonstrated in Figure 12. The carbon concentration increases by 12.3 pct when the height of the coke packed bed changes from 37 to 47 mm and

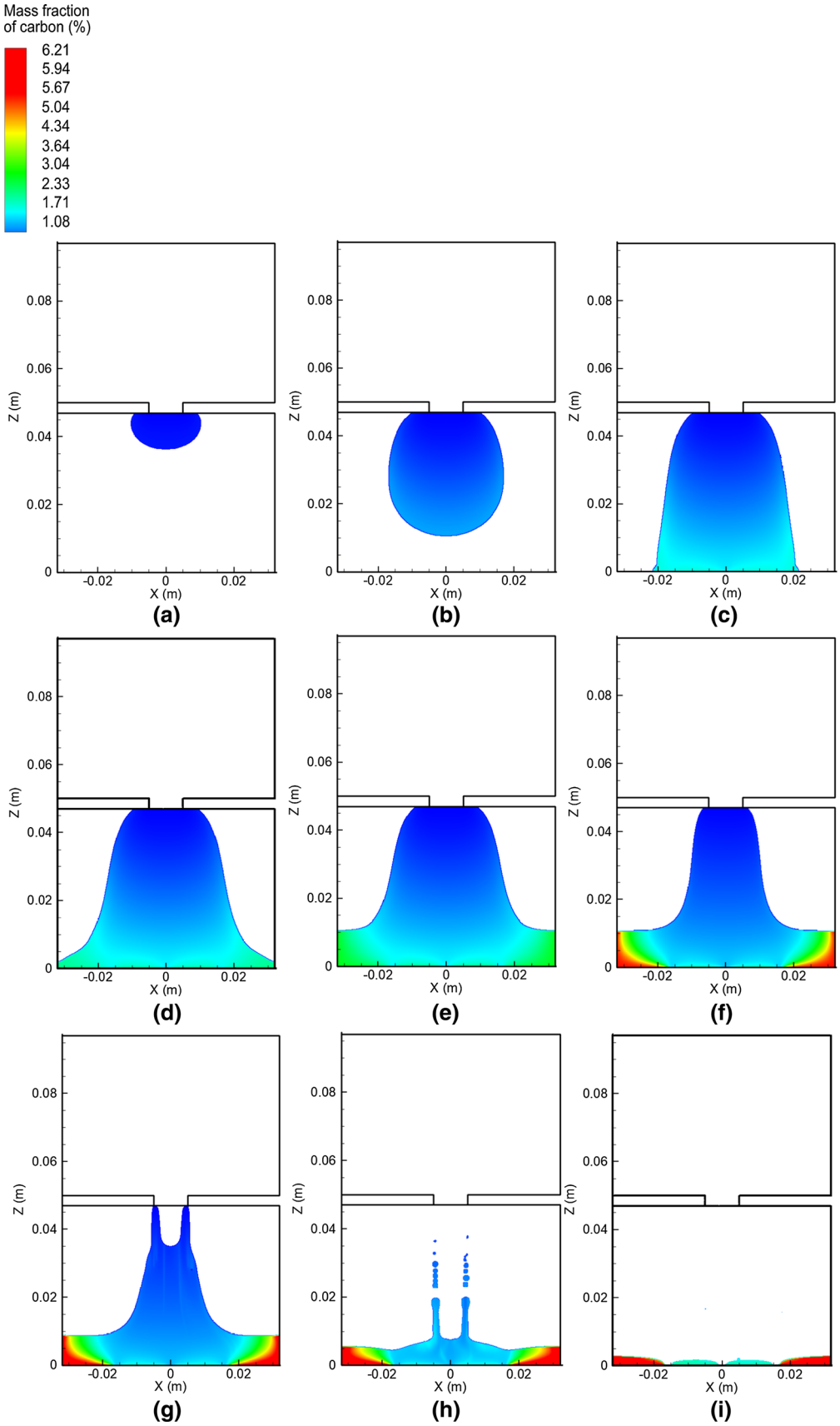
Mass fraction
of carbon (%)
6.21
5.94
5.67
5.04
4.34
3.64
3.04
2.33
1.71
1.08
Z (m)
X (m)
0.08
0.06
0.04
0.02
0
-0.02
0
0.02
(a)
(b)
(c)
(d)
(e)
(f)
(g)
(h)
(i)

◀Fig. 5—Distribution of the carbon mass fraction in the molten iron at different moments. (*a*) t_0 s, (*b*) t_0 + 0.34 s, (*c*) t_0 + 0.64 s, (*d*) t_0 + 0.84 s, (*e*) t_0 + 1.14 s, (*f*) t_0 + 2.69 s, (*g*) t_0 + 3.04 s, (*h*) t_0 + 3.54 s, and (*i*) t_0 + 4.04 s. The mean diameter of the coke is 2 mm, and the height of the coke packed bed is 47 mm.

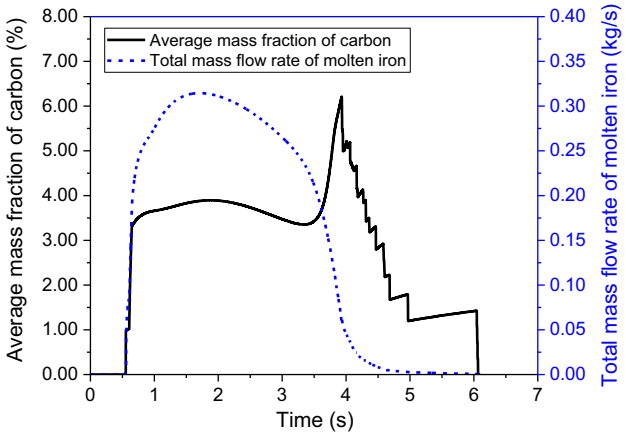

Fig. 6—Variation of the average mass fraction of the carbon and the total mass flow rate of the molten iron at the 10 outlets.

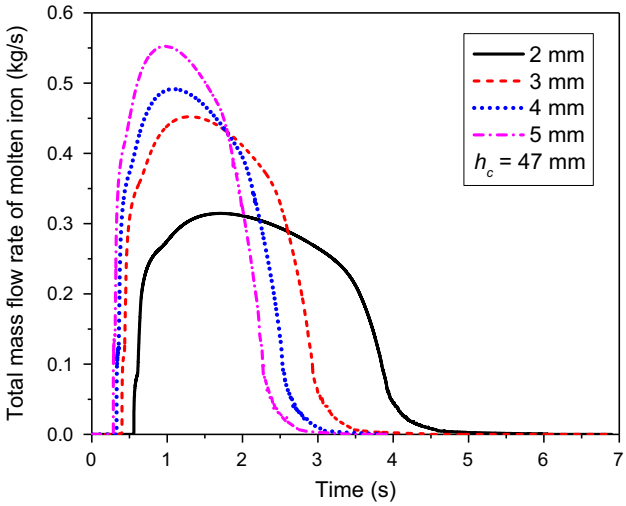

Fig. 7—Effect of the diameter of the coke on the total mass flow rate of the molten iron at the 10 outlets.

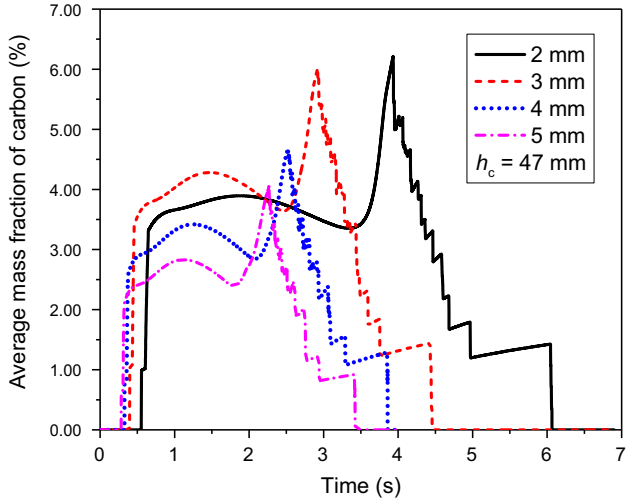

Fig. 8—Effect of the diameter of the coke on the average mass fraction of the carbon at the 10 outlets.

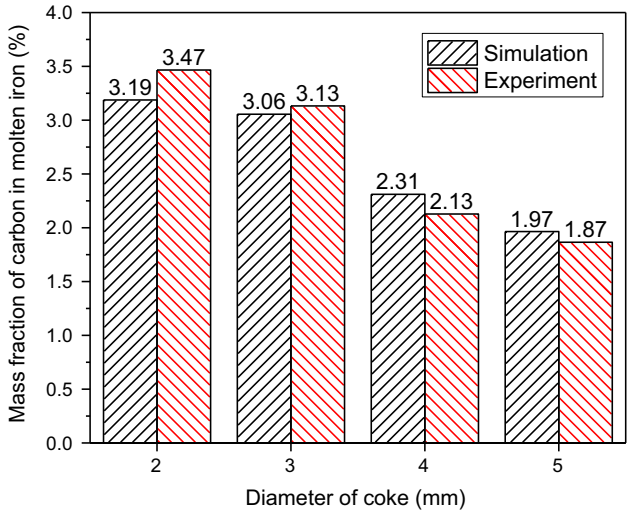

Fig. 9—Comparison of the mass fraction of the carbon in the molten iron after the carburization process with different coke diameters between the simulation and the experiment.

increases by 30.4 pct if the height of the coke packed bed continuously increases to 77 mm. The mass fraction of the carbon in the molten iron after the carburization is 4.16 pct with the 77-mm coke packed bed, which goes beyond the appropriate range, as stated previously. It can be inferred from the results that the coke packed bed with 47-mm height is enough for the carburization of the molten iron when the coke diameter is 2 mm. Additionally, the simulated results of different heights of the coke packed bed conform to the corresponding experimental results. The comparison indicates that the present model can predict the transfer behavior of the carbon with an acceptable accuracy.

Note that the parameters used in the simulation are valid only for the specified operating conditions described in the present work. It is difficult to develop a numerical model that can be used in various circumstances, since the parameters, such as rate constant and ash factor, are influenced by the device structure and operating condition. The established numerical model can be applied to the carburization process with different configurations or the large-scale industrial unit after rigorous model verification, and appropriate values of the related parameters can be evaluated according to the production data. The numerical result is able to give us deeper insight into the dripping and the carburizing behaviors of the molten iron within the coke packed bed during the flash ironmaking process.

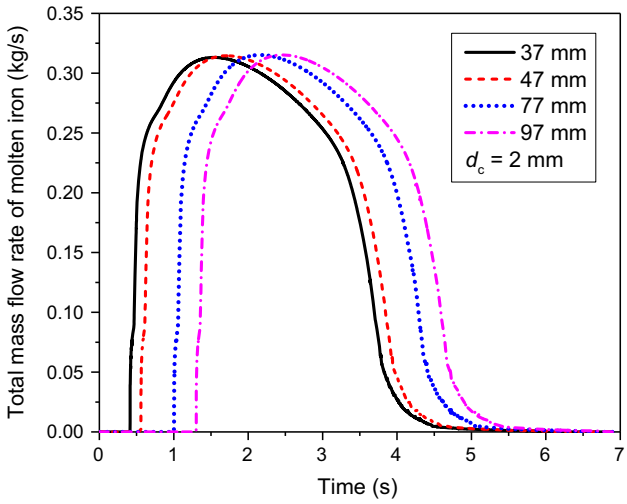

Fig. 10—Effect of the height of the coke packed bed on the total mass flow rate of the molten iron at the 10 outlets.

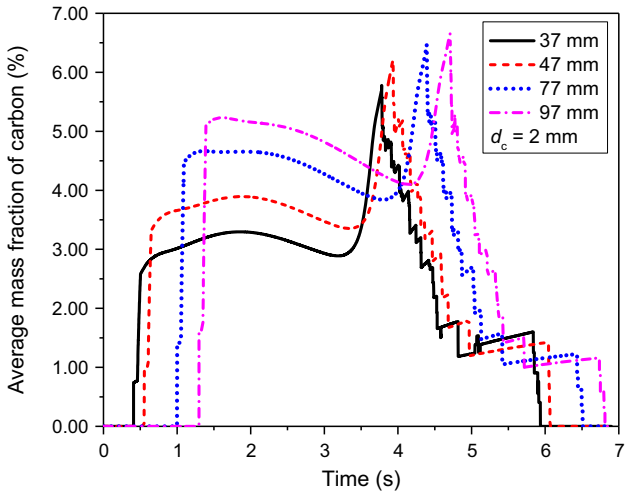

Fig. 11—Effect of the height of the coke packed bed on the average mass fraction of the carbon at the 10 outlets.

VI. CONCLUSIONS

This study established a transient three-dimensional numerical model to understand the dripping and carburizing behaviors of the molten iron within the coke packed bed during the flash ironmaking process. The influences of the diameter of the coke and the height of the coke packed bed on the mass transfer of the carbon were clarified. The VOF approach is used to describe the movement of the molten iron and the argon gas. The porous medium module is employed to define the momentum, heat, and mass transfer between the coke packed bed and the molten iron. In addition, a factor is introduced to consider the influence of the ash film on the carburization process. The solutions of all the conservation equations are simultaneously solved by the finite volume method. At the same time, a series of experiments were conducted by using a high-temperature coke packed bed for the model validation. The comparison of the experimental results and simulated

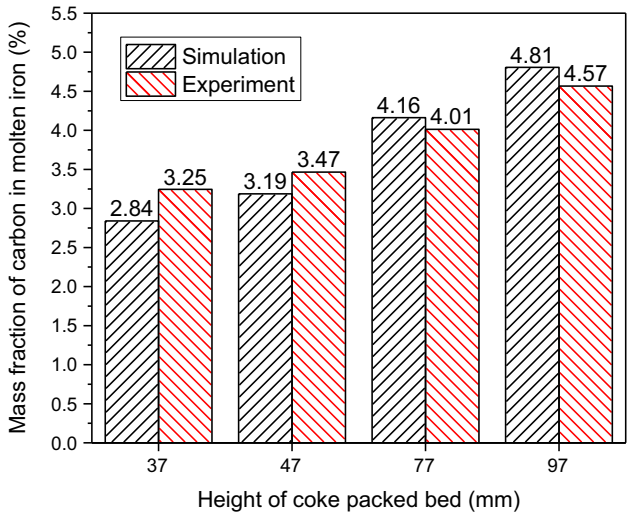

Fig. 12—Comparison of the mass fraction of the carbon in the molten iron after the carburization.

data indicates that the present model can predict the transfer behavior of the carbon with an acceptable accuracy.

The results show that the molten iron flows downward from the upper crucible to the middle crucible under the action of gravity. After entering the middle crucible, the molten iron spreads around within the coke packed bed and simultaneously moves downward. The carbon is, therefore, transferred from the coke to the molten iron. The average carbon concentration at the 10 outlets first rises fast and then enters a relatively stable period. After that, the carbon concentration increases again and a peak value of the carbon content is observed. The carbon concentration finally decreases to zero.

The residence time of the molten iron in the coke packed bed with the 47-mm height decreases from 6.03 to 3.45 seconds, while the coke diameter ranges from 2 to 5 mm. Meanwhile, the carbon concentration in the molten iron after the carburization decreases from 3.19 to 1.97 pct. With the 2-mm-diameter coke, the residence time of the molten iron in the coke packed bed increases from 5.93 to 6.79 seconds, while the height of the coke packed bed changes from 37 to 97 mm. The carbon concentration in the molten iron after the carburization, thus, increases from 2.84 to 4.81 pct. The results indicate that the 47-mm-high coke packed bed filled with the 2-mm-diameter coke can increase the carbon concentration of the molten iron to the appropriate range.

ACKNOWLEDGMENTS

The authors express their gratitude to the National Natural Science Foundation of Hubei Province, China (Grant No. 2017CFB294) and the Science and Technology Program of Beijing, China (Grant No. Z161100000716002).

REFERENCES

1. A. Hasanbeigi, M. Arens, and L. Price: *Renew. Sust. Energ. Rev.*, 2014, vol. 33, pp. 645–58.
2. W. Zhang, J.H. Zhang, and Z.L. Xue: *Energy*, 2017, vol. 121, pp. 135–46.
3. H.Y. Sohn and Y. Mohassab: *J. Sustain. Metall.*, 2016, vol. 2, pp. 216–27.
4. F. Chen, Y. Mohassab, T. Jiang, and H.Y. Sohn: *Metall. Mater. Trans. B*, 2015, vol. 46B, pp. 1133–45.
5. M.E. Choi and H.Y. Sohn: *Ironmak. Steelmak.*, 2010, vol. 37, pp. 81–88.
6. H.W. Meyer, W.F. Porter, G.C. Smith, and J. Szekely: *JOM*, 1968, vol. 20, pp. 35–42.
7. M. Ersson, L. Höglund, A. Tilliander, L. Jonsson, and P. Jönsson: *ISIJ Int.*, 2008, vol. 48, pp. 147–53.
8. H.W. Gudenau, J.P. Mulanza, and D.G.R. Sharma: *Steel Res. Int.*, 1990, vol. 61, pp. 97–104.
9. C. Wu and V. Sahajwalla: *Metall. Mater. Trans. B*, 2000, vol. 31B, pp. 243–51.
10. W.M. Husslage, M.A. Reuter, R.H. Heerema, T. Bakker, and A.G.S. Steeghs: *Metall. Mater. Trans. B*, 2005, vol. 36B, pp. 765–76.
11. D. Jang, Y. Kim, M. Shin, and J. Lee: *Metall. Mater. Trans. B*, 2012, vol. 43B, pp. 1308–14.
12. M. Shin, J.S. Oh, and J. Lee: *ISIJ Int.*, 2015, vol. 55, pp. 2056–63.
13. K. Ohno, S. Tsurumaru, A. Babich, T. Maeda, D. Senk, H.W. Gudenau, and K. Kunitomo: *ISIJ Int.*, 2015, vol. 55, pp. 1245–51.
14. S.T. Cham, V. Sahajwalla, R. Sakurovs, H.P. Sun, and M. Dubikova: *ISIJ Int.*, 2004, vol. 44, pp. 1835–41.
15. J.R. Post, T. Peeters, Y.X. Yang, and M.A. Reuter: in *2rd Int. Conf. on CFD in the Minerals and Process Industries,* Melbourne, Australia, 2003, pp. 433–40.
16. Q. Wang, F.S. Qi, Z. He, Y.W. Li, and G.Q. Li: *Int. J. Heat Mass Transf.*, 2018, vol. 120, pp. 86–94.
17. C.W. Hirt and B.D. Nichols: *J. Comput. Phys.*, 1981, vol. 39, pp. 201–25.
18. J.U. Brackbill, D.B. Kothe, and C. Zemach: *J. Comput. Phys.*, 1992, vol. 100, pp. 335–54.
19. Q. Wang, Y. Liu, F. Wang, G.Q. Li, B.K. Li, and W.W. Qiao: *Metall. Mater. Trans. B*, 2017, vol. 48B, pp. 2649–63.
20. M. Iida, K. Ogura, and T. Hakone: *ISIJ Int.*, 2008, vol. 4, pp. 412–19.
21. F. McCarthy, V. Sahajwalla, J. Hart, and N. Saha-Chaudhury: *Metall. Mater. Trans. B*, 2003, vol. 34B, pp. 573–80.
22. M.B. Mourao, G.G. Krishna Murthy, and J.F. Elliott: *Metall. Trans. B*, 1993, vol. 24B, pp. 629–37.
23. S.M. Cho, B.G. Thomas, and S.H. Kim: *ISIJ Int.*, 2018, vol. 58, pp. 1443–52.

Publisher's Note Springer Nature remains neutral with regard to jurisdictional claims in published maps and institutional affiliations.